Nereis. Revista Iberoamericana Interdisciplinar de Métodos, Modelización y Simulación	10	37-56	Universidad Católica de Valencia San Vicente Mártir	Valencia (España)	ISSN 1888-8550

Stability of Colloids in Negatively Co-operative Melittin–Phospholipid

Estabilidad de los coloides en la interacción negativa melitina-fosfolípido

Fecha de recepción y aceptación: 22 de septiembre de 2017 y 28 de diciembre de 2017

Francisco Torrens Zaragozá[1*]

[1] Institut Universitari de Ciència Molecular. Universitat de València.
[*] Correspondencia: Universitat de València. Institut Universitari de Ciència Molecular. Edifici d'Instituts de Paterna, P. O. Box 22085. 46071 Valencia. Spain. *E-mail:* torrens@uv.es.

ABSTRACT

The adsorption of melittin on 1-palmitoyl-2-oleoyl-*sn*-glycero-3-phosphocholine membranes is analysed. Rising melittin concentration, a multilayer adsorption is observed and discussed in terms of either monomer or tetramer stacking to the surface. An electrostatic adsorption model is applied because of the cationic peptide. According to the Derjaguin–Landau–Verwey–Overbeek theory, the energy well corresponding to melittin aggregation in membranes is rather broad and, practically, no barrier exists opposing the aggregation of melittin molecules. Such aggregation corresponds to a small energy variation relative to the thermal energy, which suggests that spontaneous thermal fluctuations can affect the aggregation state of melittin at the membrane–solution interface. The results of the work make evident the multilayer formation of melittin on phospholipid membranes. Melittin tetramers, which are formed in solution, bind directly to the phospholipid membrane, which results in multilayers on the surface. Adsorption is treated *via* Langmuir adsorption isotherm modified by electrostatic effects. The theoretical treatment is an elegant method because both Gouy–Chapman and Debye–Hückel formalisms apply Poisson–Boltzmann equation to calculate the potential.

KEYWORDS: *Peptide-lipid interaction*, *Thermodynamic treatment*, *Binding isotherm*, *Scatchard plot*, *Hill plot.*

RESUMEN

Se analiza la adsorción de melitina sobre membranas de 1-palmitoil-2-oleoil-*sn*-glicero-3-fosfocolina. Elevando la concentración de melitina, se observa y discute una adsorción en multicapas en cuanto a apilamiento, bien de monómeros, bien de tetrámeros, hacia la superficie. Se aplica un modelo de adsorción electrostática por el péptido catiónico. De acuerdo con la teoría Derjaguin-Landau-Verwey-Overbeek, el pozo de energía que corresponde a la agregación de melitina en membranas es bastante ancho, y prácticamente no existe barrera que se oponga a la agregación de moléculas de melitina. Tal agregación corresponde a una pequeña variación de energía relativa a la energía térmica, que sugiere que espontáneas fluctuaciones térmicas pueden afectar al estado de agregación de la melitina en la interfacie membrana-disolución. Los resultados del trabajo evidencian la formación de multicapas de melitina sobre membranas fosfolipídicas. Tetrámeros de melitina, que se forman en disolución, enlazan directamente con la membrana

fosfolipídica, que resulta en multicapas sobre la superficie. La adsorción se trata *vía* la isoterma de adsorción de Langmuir, modificada por efectos electrostáticos. El tratamiento teórico es un elegante método porque los formalismos tanto de Gouy-Chapman como Debye-Hückel aplican la ecuación de Poisson-Boltzmann para calcular el potencial.

PALABRAS CLAVE: *Interacción péptido-lípido*, *tratamiento termodinámico*, *isoterma de enlace*, *Diagrama de Scatchard*, *Diagrama de Hill*.

INTRODUCTION

Studies on the interactions between membranes and peptides are central to the knowledge of the insertion process of membrane proteins, binding of hormones to membrane receptors, and action of *antimicrobial peptides* (AMPs) and toxins. The general principles of the mechanism of interaction of surface-active peptides with membranes are understood, but the details necessary for a quantitative structure–activity and thermodynamic frameworks remain elusive. Melittin is the main active component (52 % of venom peptides) of *apitoxin* (European honey bee *Apis mellifera* venom) and is a powerful stimulator of phospholipase A2 (PLA2). It is a linear, basic, amphiphilic, cytotoxic, cytolytic and haemolytic oligopeptide with 26 amino acids (AAs) and the sequence H_3N^+–GIGAVLKVLTTGLPALISWIKRKRQQ–$CONH_2$ (molecular weight M_w=2846g·mol^{-1}). Sequences of hydrophobic (1–20) and hydrophilic (21–26) AAs are unequally distributed. It presents strong amphipathic surface activity, and is known to adopt a number of conformations and aggregation states in different aqueous solutions. Its conformation is largely *random coil* (disordered) when present as free monomer in solution. Melittin binds to cell membranes, causing their lysis *via* not completely understood mechanisms. The aggregation state and orientation of its amphipathic α–helix with respect to the membrane remain controversial. It adopts an amphipathic α–helical conformation when bound to membranes and micelles, with a flexible hinge in Pro^{14} and unordered C-terminal at 22–26 AAs. The Pro^{14} plays a critical role in its antimicrobial activity and cytotoxicity. At high peptide concentration or ionic strength, it self-associates into a tetrameric structure. The relationship between the tetrameric self-assembly of melittin and its bioactivity was linked to the necessity to prevent its hydrophobic residues from being exposed to the sugar charges present in biomembranes. Although it presents mainly hydrophobic residues, it shows six positive charges. Its N-terminal part is hydrophobic while C-end moiety is hydrophilic and strongly basic.

In order to understand membrane-lysis mechanism induced by melittin, effectors microscopic localization in the membranes at physiological concentrations is needed. Melittin orientation with respect to the bilayer surface is parallel or perpendicular, depending on the used lipid and hydration extent. Its amphiphilic nature resembles membrane-bound peptides, apolipoproteins and putative transmembrane helices of membrane proteins, which resulted in melittin being used as a model of lipid–protein interactions, toxin-mediated membrane disruption and ion channel-forming proteins. Its characteristic effect on cell membranes is the ability to lyse natural and artificial ones. It disrupts gel-phase zwitterionic 1-palmitoyl-2-oleoyl-*sn*-glycero-3-phosphocholine (POPC) membranes into small discoidal objects, with diameter of 200–400Å and a thickness of a single bilayer. In flu-

id-phase POPC bilayers, it induces the formation of large unilamellar vesicles (LUVs) with diameter of 2000Å. Because of its cationic charge, melittin binds distinctly more to anionic than zwitterionic bilayers. Studies on anions influence on melittin action were performed on binary bilayer systems of POPC and anionic lipids [*e.g*., 1-palmitoyl-2-oleoyl-*sn*-glycero-3-phosphatidylserine (PS), 1-palmitoyl-2-oleoyl-*sn*-glycero-3-phosphoglycerol (POPG)], which present the inconvenience that it is difficult to distinguish if melittin interacts with the initially provided mixture or domains locally enriched in one compound. Is glutaminyl-substrate melittin a model peptide substrate to explore membrane-phospholipids role on the enzymatic activity of tissue transglutaminase (tTGase)?

Work showed that bee venom presents multiple effects, probably as a result of its interaction with anionic phospholipids. Melittin increases the permeability of cell membranes to ions (*e.g*., Na^+, Ca^{2+}, Cl^-), which effect causes morphological (*e.g*., swelling), and functional changes in cells and tissues. Melittin exhibits antimicrobial activity *vs*. *Borrelia burgdorferi*, *Candida albicans*, *Mycoplasma hominis*, *Chlamydia trachomatis*, etc. Habermann reviewed bee and wasp venoms [1]. Properties of AMPs were reviewed [2–21]. A special issue of *Current Topics in Medicinal Chemistry* was edited on AMPs [22]. Differential AMPs interaction with lipid structures were studied by coarse-grained molecular dynamics simulations [23]. Analysis of antimicrobial activities in relation to amphipathicity and charge characterized antimicrobial peptides [24]. Work on AMP analogues from scorpion venom, antimicrobial activity and toxicity showed that α-helix interacted with biomembranes according to carpet, toroidal and barrel models, and aggregates formed with rising concentration.

In an earlier publication, it was informed the binding of vinyl polymers to anionic model membranes [25], the interaction of polyelectrolytes with oppositely charged micelles studied by fluorescence and liquid chromatography [26], the negatively co-operative binding of melittin to neutral phospholipid vesicles, the stability of pairs of colloidal particles [Derjaguin–Landau–Verwey–Overbeek (DLVO) theory] [27], the binding of water-soluble, globular proteins to anionic model membranes [28], the comparative analysis of the electrostatics of the binding of cationic proteins to vesicles, the asymmetric location of anionic phospholipids [29], the binding of mono, bi and tridomain proteins to zwitterionic and anionic vesicles, the asymmetric location of anionic phospholipids in mixed zwitterionic/anionic vesicles and the co-operative binding [30]. In *Nereis*, it was reported the polymer bisphenol-A (BPA), incorporation of silica (SiO_2) nanospheres (nanosilica, nano-SiO_2) into epoxy/amine materials, polymer nanocomposites (NCs) [31] and the calculation of restricted volume for nanoparticles that can point [32]. In the present report, the condition of DLVO stability for colloids is reviewed. The aim is to investigate if the peptide–phospholipid binding model is generally valid and determine what is the driving force for the interaction: the net surface charge density, lipid physical state or its inverse hexagonal phase (H_{II})-promoting character. The purpose is to examine the stability of thermosetting polymer/nanoclay dispersions. The main objective is to analyze the adsorption of melittin on zwitterionic lipid POPC membranes. Rising melittin concentration, a multilayer adsorption is observed and discussed in terms of monomer or tetramer stacking to the surface.

METHOD

Condition of Stability for Colloids (Derjaguin–Landau–Verwey–Overbeek Theory)

Colloids

Colloids can be classified according to the nature [gas (G), liquid (L), solid (S)] of the dispersed phase (approximately spherical fragments of size varying in 10–10^4Å) and that of the dispersive milieu. Table 1 gives some examples of colloidal systems after this classification.

Table 1. Classification of colloidal systems and examples

Class	Dispersed phase	Dispersive milieu	Examples
1. Liquid aerosols	L[a]	G	Fogs
2. Solid aerosols	S[b]	G	Fumes
3. Foams	G[c]	L	Beer
4. Emulsions	L	L	Milk
5. Colloidal suspensions (*sols*)	S	L	Paints, blood
6. Solid foams	G	S	Pumice, bread
7. Solid emulsions (*gels*)	L	S	Pearls, opal
8. Solid suspensions	S	S	Smoky glasses

[a] L: liquid.
[b] S: solid.
[c] G: gas.

The most important class, corresponding to Entry 5 (colloidal suspensions, *sols*), splits into two categories: (1) *hydrophilic (lyophilic) colloids* where properties (viscosity coefficient, surface tension) are different from the dispersive milieu (*sol* ↔ *gel*, *e.g.*, gelatine in H_2O); (2) *hydrophobic (lyophobic) colloids* where the properties look like the dispersive milieu; such colloids are p*H*-sensitive and present an instability (*flocculation*) for a p*H* higher than a critical value (*e.g.*, colloidal Au). Derjaguin–Landau–Verwey–Overbeek (DLVO) theory is devoted to lyophobic-colloids stability [33,34].

Interaction between Two Charged Spheres

The problem of the repulsive force from electrostatic origin between two charged spheres is much more difficult to solve than that of the potential originated from one charged sphere. No simple expression of the corresponding potential exists but reasonable approximations are known for limit situations [35]; *e.g.*, for two identical spheres of radius *a* in a milieu characterized by the Debye length $\lambda_D = 1/\kappa = (\varepsilon kT/8\pi e^2 n^\circ)^{1/2}$ [where ε is the solvent permittivity (before the introduction of the ions), k,

Boltzmann constant, T, the absolute temperature, e, the proton charge, and n^o, the number of ions per unit volume in the absence of any charged surface], one obtains:

$$V_{el} = \frac{\varepsilon a \psi^2}{2} \exp(-\kappa s) \tag{1}$$

where s is the shortest distance between the surfaces of the spheres in presence ($s << a$), and ψ, a potential characterizing both the charge state of the spheres and the properties of the ions of the intermediate milieu.

Total Interaction between Two Charged Spheres in an Ionized Milieu

The van der Waals (VdW) energy (attractive for two spheres presenting the same chemical composition) is:

$$V(D) = -\frac{AR}{12D} \tag{2}$$

where R is the radius of both spheres, D, the minimum distance between both spherical surfaces, A, the Hamaker constant ($A = \pi^2 n^2 B$), n, the number of spheres per unit volume, B, the attractive interaction constant of London in r^{-6} between an atom of sphere 1 and an atom of sphere 2, and r, the interatomic distance. The total interaction energy between two charged spheres in an ionized milieu is obtained, in DLVO framework, joining Eqs. (2) and (1) corresponding, respectively, to VdW and electrostatic energy (repulsive for approaching distances lower than λ_D, practically null farther). Therefore,

$$V = -\frac{Aa}{12s} + \frac{\varepsilon a \psi^2}{2} \exp(-\kappa s) \tag{3}$$

This expression will be used to discuss the stability of a colloid suspension.

Stability of a Pair of Colloidal Particles

In a colloidal suspension of *lyophobic* type, system *flocculation* is expected when the attractive forces between two particles dominate over the repulsive ones. Potential function between two charged spheres given by Eq. (3) will be written:

$$V(s) = V_A(s) + V_R(s) \tag{4}$$

Notice after Eq. (3) that absolute V_R is small with respect to V_A as for both $s \sim 0$ and $s \to \infty$. However, both cases in Fig. 1 are possible.

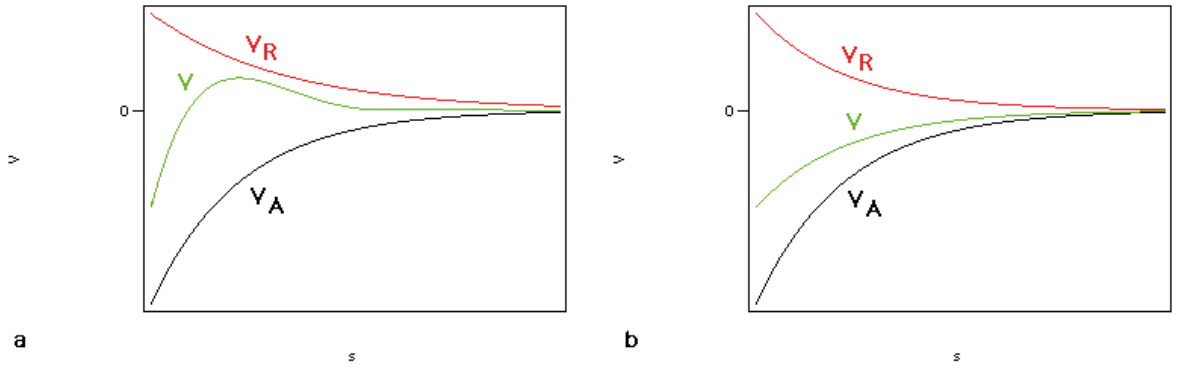

Fig. 1. Interaction potential *vs*. distance between particles: (a) domain of repulsive effects; (b) domain of attractive effects.

(1) In Fig. 1a, the repulsive effects are sufficiently intense in order that a maximum appear for $V(s)$, which corresponds to an activation energy needed for the two spheres to become in contact ($s = 0$). For a colloidal system, the figure corresponds to a possible *stability*. (2) However, in the case of Fig. 1b, V_R is too weak in order that the maximum would appear, and the figure corresponds to an immediate *flocculation* of the colloid. Figure 2 represents the net of curve $V = V(s)$ for different values of the inverse Debye length κ of the ionic milieu.

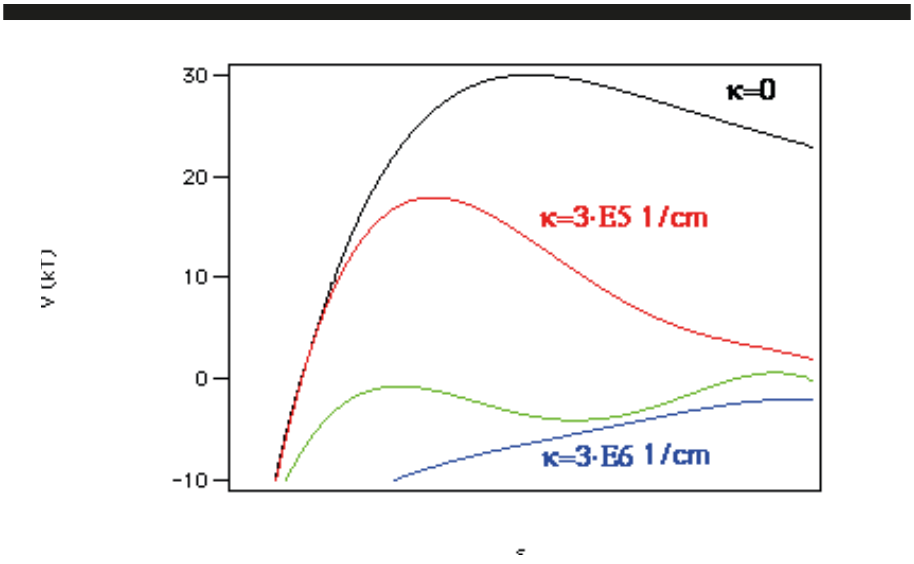

Fig. 2. Representation of the net of curve $V = V(s)$ for different values of the Debye length κ^{-1} of the ionic milieu.

One can go further searching for the condition by which curve $V = V(r)$ present a maximum and a minimum. Equation (3) can thus be rewritten, measuring s in λ_D units, *i.e.*, taking $s = \sigma/\kappa$:

$$V(\sigma) = -\frac{A\kappa a}{12\sigma} + \frac{\varepsilon a \psi^2}{2}\exp(-\sigma) \tag{5}$$

Nullifying the derivative of this expression:

$$\frac{\mathrm{d}V}{\mathrm{d}\sigma} = \frac{A\kappa a}{12\sigma^2} - \frac{\varepsilon a \psi^2}{2}\exp(-\sigma) = 0 \tag{6}$$

Thus:

$$\sigma^2 \exp(-\sigma) = \frac{A\kappa}{6\varepsilon\psi^2} \tag{7}$$

The $y(\sigma) = \sigma^2\exp(-\sigma)$ function is represented in Fig. 3.

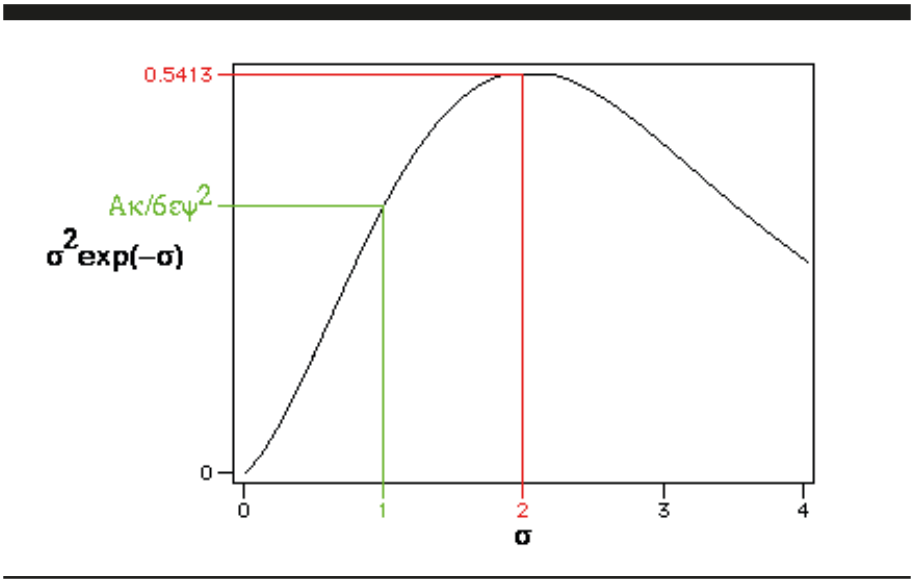

Fig. 3. Representation of the $y(\sigma) = \sigma^2\exp(-\sigma)$ function *vs*. σ.

The figure above shows that if:

$$\frac{A\kappa}{6\varepsilon\psi^2} > \frac{4}{\exp(2)} \approx 0.5413 \tag{8}$$

then $V = V(r)$ curve presents no extreme. In this case, the attractive VdW force dominates, whichever s be, over the electrostatic repulsion and the colloid is *unstable*. Inequality (8) can also be written:

$$\psi^2 < \psi_{crit}^2 = \frac{A\kappa}{24\varepsilon}\exp(2) \tag{9}$$

For a millimolar aqueous solution of monovalent ions, one has $\psi_{crit} = 19$mV. When $V = V(r)$ presents a maximum, *i.e.*, if $\psi > \psi_{crit}$, one can search for the value of V that correspond to the maximum. It matches to a value of σ_o of σ so that:

$$\exp(-\sigma_o) = \frac{A\kappa}{6\varepsilon\psi^2\sigma_o^2} \tag{10}$$

From which:

$$V(\sigma_o) = -\frac{A\kappa a}{12\sigma_o} + \frac{\varepsilon a\psi^2}{2}\exp(-\sigma_o) = -\frac{A\kappa a}{12\sigma_o} + \frac{A\kappa a}{12\sigma_o^2} = \frac{A\kappa a}{12\sigma_o}\left(\frac{1}{\sigma_o} - 1\right) \tag{11}$$

Let us assume $\psi >> \psi_{crit}$, then $\sigma_o^2\exp(-\sigma_o) = A\kappa/(6\varepsilon\psi^2) << 1$, and $\sigma_o << 1$. From which:

$$V(\sigma_o) \approx \frac{A\kappa a}{12\sigma_o^2} = \frac{\varepsilon a\psi^2}{2} \tag{12}$$

For instance, if $a = 0.5\mu$m, $\varepsilon_w = 80$ (aqueous solution, $\varepsilon = \varepsilon_w\varepsilon_o = 7\text{x}10^{-10}\text{C}^2\cdot\text{N}^{-1}\cdot\text{m}^{-2}$), $\psi = 100$mV, then $V(\sigma_o) = 2.2\cdot10^{-17}$J. At room temperature (RT) one obtains:

$$\frac{V(\sigma_o)}{kT} \approx 5000$$

In the conditions above, the activation energy is 5000 times higher than the average thermal agitation energy. One can then consider that one collision out of $\exp(5000) \approx 10^{2000}$ will cause the co-alescence of the two concerned colloidal particles. The suspension could then be considered stable (*flocculation* of the colloid cannot occur).

Stability of Thermosetting Polymer/Nanoclay Dispersions

The term *stability* presents two meanings in the context of colloidal dispersions. In practice, it is used to show that there is no phase separation during a period. If the particles in a dispersion show a trend to sediment during an episode of storage, the dispersion is unstable. However, in another context, the word *stability* is utilized when the particles do not show a tendency to aggregate. The key to understand the expression *colloidal stability* is in the pair of potentials existing between two parti-

cles. The colloidal particles are subjected to attraction and repulsion forces, and an equilibrium exists between such forces. Brownian motion produces collision between the particles and, if the attraction forces dominate, the particles agglomerate after the impact. On the contrary, if the repulsion forces prevail, the particles remain separate after the collision. The attraction forces are those of VdW, while the repulsion forces come from the interaction between the electric double layers that enclose the particles. Variations of milieu ionic strength or p*H* modify electrostatic forces, which allows controlling co-agulation processes. Theory of DLVO developed the research, which gives total potential V_T as:

$$V_T = V_A + V_R \tag{13}$$

where V_T is total potential between two particles as the addition of attraction V_A and repulsion V_R potentials. The curve that represents the total energy of interaction between colloidal particles (V_T) is the adding of attraction (V_A) and repulsion (V_R) curves. It corresponds to an exponential equation, because repulsion force is inversely proportional to the square of distance, and the attraction force is also a function of the inverse of distance but this raised to an exponent always greater than two. When the attraction by VdW forces is greater than the electrostatic repulsion, one is in the primary minimum potential (*cf*. Fig. 4), which indicates the aggregation state of the particles with the condition of minimum energy. The state of primary maximum represents the activation energy necessary to reach the aggregation state. Movement of the particles is governed by the thermal energy and, naturally, one can describe the energy distribution after Boltzmann equation. One can predict the kinetic stability as aggregation rate, being proportional to: $\exp(-V_T/k_BT)$. When $V_T >> k_BT$, the particles will be in a *stable* colloidal state. If the attraction energy is slightly greater than the thermal energy average, the aggregation states will be reversible (secondary minimum state). If a strong attraction exists between the particles, one has $-V_T >> k_BT$, and get a strong aggregation or *co-agulation* of the particles, resulting the process irreversible (primary minimum state).

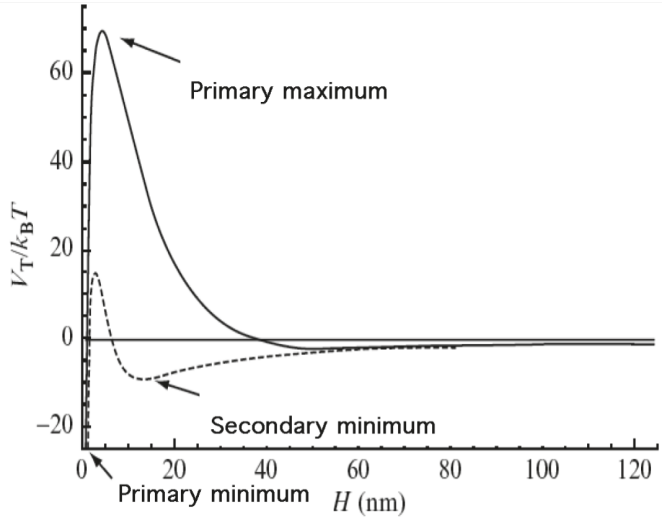

Fig. 4. Interaction potential *vs*. distance between the particles.

On rising particle concentration in the milieu, the aggregates grow in size, adopting a fractal-type structure. Russel *et al*. described the phenomenon [36]. The aggregates grow and occupy the whole available space. In this point, the *percolation threshold* is reached. When rising particle concentration, the aggregates grow forming clusters that, in turn, interact with one another producing a continuous structure crosslinked (*net*) in three dimensions (3D). From this point, on rising particle concentration, dense structures are formed, which are more difficult to describe from an only parameter, *e.g*., fractal dimension. *Gelification* corresponds, at the molecular level, to the incipient formation of branched and reticulated molecules of a molecular weight that tends to infinite, insoluble and infusible. When *gelification* occurs, the system passes from liquid to a covalently interwoven *gel*. The phenomenon is associated with a sharp rise in the viscosity coefficient. From the theoretical viewpoint, the *gel* point was described *via* predictions of the classical polymerization theory developed by Flory [37] to modern fractal geometry [38] and percolation theory [39]. The theories contributed different explanations for the critical transition. Flory theory is incomplete because it does not consider the formation of rings, which implies that the mass of the fractal set rises with the fourth power of size, which is not realistic. Percolation theory allows the formation of rings, or closed cycles, so that it does not predict a divergent density for the fractal set. The validity of percolation theory lies in its ability to predict the behaviour of certain physical properties near the *gel* point [storage (elastic) modulus, viscosity coefficient, cluster average size and size distribution, *gel* volume fraction, etc.] *via* scaling laws governed by critical exponents. Fractal geometry is based on a structure invariant to scale (a part is structurally identical to the total) and shows a decay in density with the rise in aggregates size. Fractal objects are characterized by their fractal dimension *D*, which is defined from the fractal mass and surface by the following relationships:

$$M \sim R^{D_m} \qquad S \sim R^{D_s} \tag{14}$$

where *M* and *S* are the object mass and surface, and *R*, its average size. Fractal mass and surface can never be in the same length scale. Index D_m takes values in 1–3. The values result from D_m = 1–1.5, which corresponds to a long linear polymer, passing by D_m = 1.5–2.25 for branched and dendritic polymers to dense aggregates with $D_m \sim 3$. On the other hand, the values of D_s rise from $D_s \sim 2$ for a smooth surface to $D_s \sim 3$ for a wrinkled surface. Shih *et al*. theory (1990) explained the formation of a continuous colloidal structure, crosslinked by interaction between the fractal flocs, distinguishing between two regimes according to colloidal-*gel* concentration [40,41]. It is important to determine the dependence of the storage shear modulus *G'* on clay volume fraction ϕ, in order to understand the mechanism controlling *net*-structure formation. Depending on the strength of the links between the flocs in comparison to that of the flocs, two regimes occur.

(1) *Strong-link* regime, where:

$$G' \sim \phi^{(d+x)/(d-D)} \tag{15}$$

where *d* is the Euclidean dimension, *D*, fractal dimension of the flocs, and *x*, backbone fractal dimension (chemical length exponent, tortuosity) of the flocs ($1 \leq x < D$). The *limit of linearity* (*critical strain*):

$$\gamma_c \sim \phi^{-(1+x)/(d-D)} \tag{16}$$

(2) *Weak-link* regime, where:

$$G' \sim \phi^{(d-2)/(d-D)} \tag{17}$$

and

$$\gamma_c \sim \phi^{1/(d-D)} \tag{18}$$

In the strong-link regime, the interaction force between the flocs overcomes the interaction forces from inside the same floc while, in the weak-link regime, the interaction force between the particles from inside the same floc overwhelms the forces between the flocs. The main differences between the two regimes are: (1) *G'* rises more slowly in the weak- than in the strong-link regime; (2) the limit of linearity γ_c rises with increasing particle concentration in the weak-link regime but decays with rising particle concentration in the strong-link regime. Extensions to the DLVO theory were informed. Bocquet *et al*. reported effective charge saturation in colloidal suspensions [42]. Chapot *et al*. published interaction between charged anisotropic macromolecules and applied it to rod-like polyelectrolytes [43].

RESULTS

The use of the partition equilibrium model, in combination with Gouy–Chapman formalism, provided an expression to generate theoretical association isotherms that depended on two adjustable parameters: (1) the theoretical partition coefficient Γ, calculated from the initial slope of the experimental curves; (2) the peptide effective interfacial charge ν. The experimental binding isotherms were fitted *via* Γ and ν parameters. The theoretical isotherms looked qualitatively similar to those obtained *via* the thermodynamic approach. Values of Γ theoretically calculated for melittin were of the same order of magnitude than those derived from the fitting analysis, which means that for every binding isotherm, the evaluated actual peptide charge in solution z_p^+ originated a theoretical Γ value similar to that obtained from the initial slope. However, with the present thermodynamic treatment, the determination of Γ and ν parameters was made separately, without any extrapolation from the experimental isotherm. Data on multilayer formation of melittin on solid-supported POPC membranes (*cf*. Table 2) show a small calculated surface charge density σ in the range 0–12mC·m^{-2}, too small to avoid co-alescence [44]. Surface potential ψ_o calculated *via* Gouy–Chapman theory lies in the range 0–16mV. As a first approximation, a value of ionic strength (*I*)-corrected water permittivity $\varepsilon_w = 77.3062 - 13.1601I = 76.8$ and α–helix conformation for the peptide (disc surface charge distribution,

$a = R_p$ = 7Å [45]) were used. It was shown by spectroscopy that in the presence of membrane-mimetic solvents and/or surfactantants, melittin formed a partial α–helix [46–48]. The DLVO analysis allows calculating an activation energy for co-alescence in the range of 0–38J·mol^{-1} or 0–0.02 units of kT at room temperature (T = 25 °C), which indicates that one collision of 1–1.02 will cause the co-alescence of adsorbed melittin molecules, which is in agreement with the fact that melittin aggregates in membranes predominantly in the form of tetramers. This supports the scenario of multilayer formation in which melittin tetramers, which are formed in solution, bind directly to the phospholipid membrane, which turns out to be in multilayers (double layers) on the surface, which is in contrast to observations with DOPC vesicles [49], confirming the importance of the experimental conditions [concentration of melittin, pH, temperature, ionic strength (salt concentration), etc.].

Table 2. Melittin–POPC binding (temperature T = 25 °C, ionic strength I = 0.04mol·L^{-1}, pH 7.2)

c_p^{A} [a] (μmol·L^{-1})	α/R_i [b] (mmol·mol^{-1})	σ [c] (mC·m^{-2})	ψ_o [d] (mV)	c_p^{o} [e] (μmol·L^{-1})	K_p [f] (L·mol^{-1})	V [g] (J·mol^{-1})	V/kT [h]	Exp(V/kT) [i]
0.00	0.00	–	–	–	–	–	–	–
1.60	4.40	2.25	3.4	1.2	3670	2	0.0007	1.0007
2.2	3.60	1.8	2.8	1.7	2080	1	0.0005	1.0005
3.8	5.54	2.8	4.2	2.7	2090	3	0.001	1.001
6.2	7.54	3.8	5.7	3.8	1980	5	0.002	1.002
7.3	8.18	4.1	6.1	4.3	1900	5	0.002	1.002
8.4	9.78	4.9	7.2	4.5	2170	7	0.003	1.003
11.2	12.08	6.1	8.8	5.3	2290	11	0.004	1.004
20.5	16.4	8.1	11.5	7.6	2150	19	0.008	1.008
26.8	18.9	9.3	13.0	8.8	2150	24	0.01	1.01
40.2	23.2	11.3	15.4	10.7	2170	34	0.01	1.01
66.9	24.8	11.9	16.2	16.6	1490	38	0.02	1.02

[a] Equilibrium melittin concentration in the bulk solution.
[b] Moles of bound melittin per mole of POPC.
[c] Surface charge density calculated according to Seelig, Allegrini and Seelig with A_L = 68Å^2, A_p = 200Å^2, and z_p^+ = 2.2 e.u.
[d] Surface potential calculated by means of Gouy–Chapman theory.
[e] Concentration of melittin at the binding plane calculated with z_p^+ = 2.2 e.u.
[f] Partition coefficient.
[g] Activation energy calculated with ionic strength-corrected water permittivity ε_w = 76.8 and a = 7Å.
[h] Activation energy in kT units, where k is Boltzmann constant.
[i] Number of collisions necessary for achieving one effective collision.

DISCUSSION

The adsorption of melittin on phospholipid vesicles is treated *via* Langmuir adsorption isotherm modified with electrostatic effects [50]. The theoretical approach is an elegant treatment, because the

two Gouy–Chapman and Debye–Hückel formalisms applied the same Poisson–Boltzmann equation to calculate either potential [51]. On comparing the adsorption of cationic melittin on zwitterionic and anionic phospholip vesicles, the latter is more complex because of its greater cover of the surface, which allows raising three questions: (1) Does the phospholipid surface continue to be anionic after a great cover by the cationic peptide? (2) What is the actual charge of the anionic surface after the adsorption of the cationic peptide? (3) Is Langmuir-modified adsorption isotherm still valid? The theoretical association isotherms, generated from the values of the actual peptide charge in solution z_p^+, described satisfactorily the experimental data at lower ionic strength, and a number of parameters, included in the equation, were varied in order to better reproduce the experimental binding curves obtained at higher ionic strengths. The partition coefficient theoretically derived for melittin was similar to that deduced according to more classical binding analyses. The formalism allowed determining the values of the molar free energies for melittin in aqueous and lipid phases. Such an understanding of the thermodynamic parameters provided interesting information about the energetic of the peptide–lipid interactions. In the following, I shall provide a tentative model for the topology of melittin in two possible scenarios of multilayer formation on POPC membranes. A thermodynamic approach was proposed to analyse quantitatively the binding isotherms of peptides to model membranes *vs*. one adjustable parameter: z_p^+. The main features of the treatment were: (1) a theoretical expression for the partition coefficient calculated from the molar free energies of the peptide in both aqueous and lipid phases; (2) an equation proposed by Stankowski to evaluate the activity coefficient of the peptide in the lipid phase; (3) Debye–Hückel equation that quantifies the activity coefficient of the peptide in the aqueous phase [52]. In order to assess the validity of the method, the interaction of basic amphipathic peptides was studied *via* steady-state fluorescence spectroscopy, which provides: (1) intensity (related to the abundance of the melittin–peptide complex); (2) blueshift (penetration of the hydrophobic part of melittin in the bilayer). The obtained z_p^+ charges were always found to be lower than the electrostatic charge expected from the number of ionizable groups in the cationic peptide (q = 6 e.u.) [53]. The z_p^+ charges were rationalized, considering that the peptide charged groups were strongly associated with the counterions in the buffer solution at a given ionic strength [54]. The partition coefficients theoretically derived *via* z_p^+ charges were in agreement with those deduced from Gouy–Chapman formalism [55]. From z_p^+ charges, the molar free energies for both free and lipid-bound states of the peptides were calculated.

The experimental activity coefficient was explained taking into account the electrostatic effects and ν charge, and the experimental binding isotherms were fitted *via* Γ and ν parameters [56]. However, determined ν charges were also smaller than the electrostatic charge of the cationic peptide, which observation was understood when it was considered that the actual z_p^+ charge of the cationic polypeptide should decay, because of the screening effect of the counterions in the electrolyte solution, which provided a given ionic strength [57]. In order to explain the charge difference, theoretical treatments were reported, but the thermodynamic parameters involved in the peptide–surface interactions were not well defined for electrolytes greater than 1:1 [58]. A thermodynamic approach was proposed for the quantitative analysis of the peptide/lipid-surface binding isotherms. The treatment was based on the partition equilibrium model and introduced: (1) the theoretical expressions for the quantitative calculation of the molar free energies of the peptide in both aqueous and lipid phases, which allowed the evaluation of the partition coefficient; (2) the calculation of the activity coefficient

via concepts from the virial approach and Debye–Hückel theory, with both disc and hemispheric surface charge distributions considered for the peptide/vesicle contact. All the proposed expressions were based on the knowledge of the actual peptide charge in solution z_p^+, which was different from the electrostatic charge of the cationic peptide. Once z_p^+ charge was known, ν charges were derived *via* Gouy–Chapman theory. With the present thermodynamic treatment, the determination of theoretical partition coefficient Γ and ν charge parameters was made separately, without any extrapolation from the experimental binding isotherm, which observation was understood when it was considered a disc surface charge distribution for the melittin/vesicle contact.

Some amount of high-molecular mass complexes of melittin with mainly anionic phospholipids existed. The interaction between cationic melittin and POPC vesicles/membranes presented four phases. (1) The initial interaction between melittin and vesicles/cells was merely electrostatic *via* the basic C-terminus, but melittin was not fully stabilized at the vesicle/membrane plane and remained in a low α–helical conformation. (2) The next step after the electrostatic interaction was a melittin stabilization in the vesicle/membrane. Conformational changes were induced to yield a peptide–lipid complex showing the lowest possible energy state. (3) The insertion of melittin in the vesicle/bilayer induced a re-organization of the vesicle/membrane components, which facilitated the cytoplasm release and concomitant cell collapse. (4) After the lysis was completed, melittin was complexed with mainly anionic phospholipids. The agreement between the results, obtained with wasp venom peptide toxin mastoparan, and experimental results gotten for melittin and neuropeptide substance *P*, supported that quantitative studies of the binding of amphipathic peptides to zwitterionic and anionic phospholipid membranes were achieved, *via* the thermodynamic approach, especially at lower ionic strength. However, at higher salt concentration, the thermodynamic treatment did not completely predict the shape of the curves at high surface cover, which was attributed to the fact that an average z_p^+ charge was assumed in all cases in the calculations, as representative of the whole adsorption isotherm. At lower ionic strength, z_p^+ charges in every point of the adsorption isotherm were similar and an average $<z_p^+>$ charge were adequate. Notwithstanding, at higher salt concentration, z_p^+ charges calculated for every experimental datum in the corresponding adsorption isotherm varied slightly, and the average z_p^+ charge was considered as a less representative parameter of the whole adsorption isotherm, which could be corrected introducing, in the theoretical expression of the molar free energies of the peptide in both aqueous and lipid phases, additional terms accounting for the interaction between the free peptide and the counterions present in the solution.

Figure 5 shows the schematic representation of two possible scenarios of multilayer formation. The *cylinders* represent the melittin molecules. In Figure 5a, melittin tetramers, which were formed in solution, bound directly to the phospholipid membrane, which resulted in multilayers (double layers) on the surface. In Figure 5b, although at higher melittin concentrations tetramers existed in solution, only monomers bound to the surface, forming multilayers. Data on multilayer formation of melittin on solid-supported POPC membranes, especially the small calculated surface charge density σ in the range 0–12mC·m^{-2}, was too small to avoid co-alescence, in agreement with the evidence for multilayer formation of melittin on solid-supported phospholipid membranes by shear-wave resonator measurements.

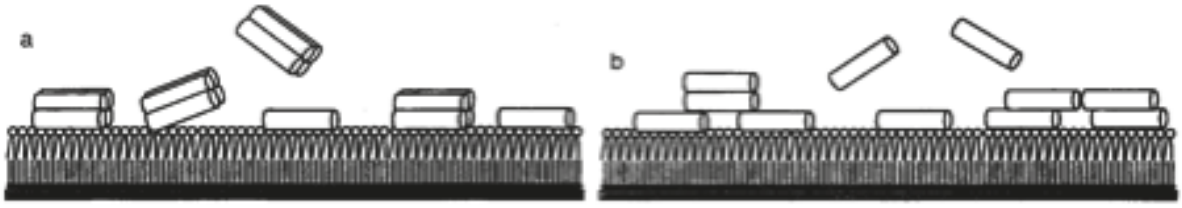

Fig. 5. Two scenarios of multilayer formation: (a) tetramers; (b) monomers. *Cylinder*: melittin. Modified from Ref. [44].

The local microenvironment composition of the lipid bilayer played a role as a regulator of the cross-linking activity of melittin and other toxins. In anionic phospholipid bilayers, its physical state *gel* or *liquid crystal* had no effect on melittin binding, contrary to neutral lipids, which showed that electrostatic forces played a role in the formation of the complex, and ruled out a penetration of the hydrophobic part of the peptide in the bilayer. The conclusion is supported by the fact that the stoichiometry of complexes was related to the surface charge density of the bilayer, as shown by p*H* effects on dimyristoylphosphatidic acid. The physical state of the bilayer and hydrophobic force played a role in the interaction with the toxins. However, at variance to neutral membranes, the driving force was modulated by electrostatic interactions, which controlled the phase formation below or above the temperature of gel-to-fluid transition. In addition to the interest in cell membranes and phospholipid bilayers, motivation exists for the design of supported membrane biosensors for medical and pharmaceutical applications. Assuming a certain structure for colloidal gels, a simple but systematic scaling theory was derived for storage modulus and limit of linearity of colloidal gels that were above the *gelation* threshold. The scaling of the elastic properties of colloidal gels resulted dominated by the fractal nature of the flocs and different from the scaling near the gelation threshold, where a percolation-type scaling applied. The exponents for storage modulus and limit of linearity were expressed in terms of flocs and backbone fractal dimensions. Flocs fractal dimension resulted that of the colloidal aggregates. Two types of scaling behaviour existed: strong- and weak-link regimes. The scaling of the storage modulus and limit of linearity depended on whether the interfloc links were stronger than the flocs. The linear region shrunk with the rising concentration in the strong-link regime but rose with the rising concentration in the weak-link scheme. The theory enabled extracting, from the rheological measurements, structural information about the individual flocs. The fractal dimension of the microstructural net of a fat crystal net is an indicator of the storage modulus of the net and hardness of the fat crystal net. The fractal and fractal backbone dimensions were calculated from polarized light microscope images of the net. The AMPs showed *in vitro* activity *vs*. micro-organisms resistant to conventional antibiotics. Their most common mode of action was the disruption of cell membranes leading to microbial lysis, which presented lesser risk of acquired resistance or cross-resistance with other agents than other modes, which made it an attractive template for the design of antimicrobials for specific applications. The outmost leaflets of the bilayer, which is exposed to the outside of the anionic bacterial membranes, are more attractive to the attack of cationic AMPs. The interaction is

mainly electrostatic actions, which are the major driving forces for cellular association. A need exists for modernizing the statistical methods used in research. Statistical modelling is improving. One cannot be an expert in everything; however, one can be encircled by experts. Is statistics a noble branch of esoteric sciences or an instrument to clarify a phenomenon existing behind data? Is the statistician a being nonplussed to a computer or an active collaborator integrated into a research team? New statistical methods allow to get more robustness in the conclusions and extract more information from the data.

CONCLUSION

From the previous results and discussion, the following conclusions can be drawn.

1. According to the Derjaguin–Landau–Verwey–Overbeek model, the energy well corresponding to melittin aggregation in membranes was rather broad and, practically, no barrier exists opposing the aggregation of melittin molecules. Such aggregation corresponds to a small energy variation relative to thermal energy, which suggested that spontaneous thermal fluctuations affected melittin aggregation state at membrane/solution interface. The adsorption was treated *via* Langmuir adsorption isotherm modified with electrostatic effects. The theoretical treatment was an elegant method, because the two Gouy–Chapman and Debye–Hückel formalisms applied the same Poisson–Boltzmann equation to calculate either potential.

2. The results made evident the formation of the melittin multilayer on the phospholipid membranes. Melittin tetramers, which were formed in solution, bound directly to the phospholipid membrane, which resulted in multilayers on the surface. Work is in progress on testing the utility of steady-state spectrofluorimetry, Förster resonance energy transfer, fluorescence anisotropy and polarization, total internal reflection fluorescence, circular dichroism, circular-dichroic stopped-flow, polarimetry, Raman spectroscopy, polarized and attenuated total reflection Fourier-transform infrared spectroscopy, infrared dichroism, sum frequency generation vibrational spectroscopy, ^{31}P, ^{13}C, ^{1}H, ^{2}H, spin label, solid-state, nuclear-Overhauser, photochemically induced dynamic-nuclear-polarization and heteronuclear single-quantum coherence nuclear magnetic resonance, electron spin-echo envelope modulation and resonance spectroscopy, quasi-elastic light scattering, thin-layer, reverse-phase and size-exclusion high-performance liquid chromatography, X-ray diffractometry, X-rays and neutron off-plane scattering, electron and confocal microscopy, high-sensitivity differential scanning calorimetry, temperature scanning densitometry, conductance, viscometry, ultracentrifugation, quartz crystal microbalance, lateral diffusion measurements, imaging ellipsometry, reflection interference contrast microscopy, enzymatic cleavage experiments, cytolytic and haemolytic activity assays, assay of antibacterial activity of the peptides, fractal dimension analysis, molecular dynamics simulations, molecular modelling and computer analysis to confirm the present outcomes.

3. Further work will give a better quantitative description of the association isotherms at higher ionic strength and improve the approach in anionic lipid membranes. Although melittin enlightened its behaviour in the presence of natural membranes, it still remains to settle more definitively the parallelism between its perturbation induced on lipids and cell membranes. What is the detailed structure

of the detected *soluble* complexes? To which extent are they involved in the mechanism of action of cytolytic toxins?

ACKNOWLEDGEMENT

The author wants to dedicate this manuscript to Prof. Dr. Agustín Campos, who was greatly interested in this research and would have loved to see its conclusion. He acknowledges financial support from Universidad Católica de Valencia San Vicente Mártir (Project No. UCV.PRO.17-18.AIV.03).

LITERATURE CITED

[1] Habermann E. Bee and wasp venoms. Science 1972;177:314-22.
[2] Nicolas P, Mor A. Peptides as weapons against microorganisms in the chemical defense system of vertebrates. Annu. Rev. Microbiol. 1995;49:277-304.
[3] Kourie JI, Shorthouse AA. Properties of cytotoxic peptide-formed ion channels. Am. J. Physiol. Cell Physiol. 2000;278:C1063-87.
[4] Brogden KA. Antimicrobial peptides: Pore formers or metabolic inhibitors in bacteria? Nat. Rev. Microbiol. 2005;3:238-50.
[5] Sundriyal S, Sharma RK, Jain R, Bharatam PV. Minimum requirements of hydrophobic and hydrophilic features in cationic peptide antibiotics (CPAs): Pharmacophore generation and validation with cationic steroid antibiotics (CSAs). J. Mol. Model. 2008;14:265-78.
[6] Zhou X, Li Z, Dai Z, Zou X. QSAR modeling of peptide biological activity by coupling support vector machine with particle swarm optimization algorithm and genetic algorithm. J. Mol. Graphics Model. 2010;29:188-96.
[7] Eckert R Road to clinical efficacy: Challenges and novel strategies for antimicrobial peptide development. Fut. Microbiol. 2011;6:635-51.
[8] Fjell CD, Jenssen H, Cheung WA, Hancock REW, Cherkasov A. Optimization of antibacterial peptides by genetic algorithms and cheminformatics. Chem. Biol. Drug Des. 2011;77:48-56.
[9] Kosciuczuk EM, Lisowski P, Jarczak J, Strzalkowska N, Józwik A, Horbanczuk J, Krzyzewski J, Zwierzchowski L, Bagnicka E. Cathelicidins: Family of antimicrobial peptides. A review. Mol. Biol. Rep. 2012;39:10957-70.
[10] Galdiero S, Falanga A, Cantisani M, Vitiello M, Morelli G, Galdiero M. Peptide–lipid interactions: Experiments and applications. Int. J. Mol. Sci. 2013;14:18758-89.
[11] Forbes S, McBain AJ, Felton-Smith S, Jowitt TA, Birchenough HL, Dobson CB. Comparative surface antimicrobial properties of synthetic biocides and novel human apolipoprotein E derived antimicrobial peptides. Biomaterials 2013;34:5453-64.
[12] Gomes-Neto F, Valente AP, Almeida FCL. Modeling the interaction of dodecylphosphocholine micelles with the anticoccidial peptide PW2 guided by NMR data. Molecules 2013;18:10056-80.

[13] Imran S. Studies on the antibacterial peptide isolated from *Murrya konigii* leaves. Res. J. Biotechnol. 2013;8(12):49-53.
[14] Ryu S, Song PI, Seo CH, Cheong H, Park Y. Colonization and infection of the skin by *S. aureus*: Immune system evasion and the response to cationic antimicrobial peptides. Int. J. Mol. Sci. 2014;15:8753-72.
[15] Vale N, Aguiar L, Gomes P. Antimicrobial peptides: A new class of antimalarial drugs? Front. Pharmacol. 2014;5:275–1-13.
[16] Tan J, Huang J, Huang Y, Chen Y. Effects of single amino acid substitution on the biophysical properties and biological activities of an amphipathic ahelical antibacterial peptide against Gram-negative bacteria. Molecules 2014;19:10803-17.
[17] Dziuba B, Dziuba M. New milk protein-derived peptides with potential antimicrobial activity: An approach based on bioinformatic studies. Int. J. Mol. Sci. 2014;15:14531-45.
[18] Chifiriuc MC, Grumezescu AM, Lazar V, Bolocan A, Triaridis S, Grigore R, Bartesteanu S. Contribution of antimicrobial peptides to the development of new and efficient antimicrobial strategies. Curr. Proteom. 2014;11:98-107.
[19] Duncan V, Fraser-Pitt D, Mercer D. First class. Eur. Biopharm. Rev. 2014;2014(66):56-9.
[20] Lee G, Bae H. Antiinflammatory applications of melittin, a major component of bee venom: Detailed mechanism of action and adverse effects. Molecules 2016;21:616–1-10.
[21] Primon-Barros M, Macedo AJ. Animal venom peptides: Potential for new antimicrobial agents. Curr. Top. Med. Chem. 2017;17:1119-56.
[22] Dawgul M. Antimicrobial peptides. Curr. Top. Med. Chem. 2017;17:507.
[23] Balatti GE, Ambroggio EE, Fidelio GD, Martini MF, Pickholz M. Differential interaction of antimicrobial peptides with lipid structures studied by coarse-grained molecular dynamics simulations. Molecules 2017;22:1775–1-17.
[24] Wang CK, Shih LY, Chang KY. Large-scale analysis of antimicrobial activities in relation to amphipathicity and charge reveals novel characterization of antimicrobial peptides. Molecules 2017;22:2037–1-8.
[25] Torrens F, Campos A, Abad C. Binding of vinyl polymers to anionic model membranes. Cell. Mol. Biol. 2003;49:991-8.
[26] Torrens F, Abad C, Codoñer A, García-Lopera R, Campos A. Interaction of polyelectrolytes with oppositely charged micelles studied by fluorescence and liquid chromatography. Eur. Polym. J. 2005;41:1439-52.
[27] Torrens F, Castellano G, Campos A, Abad C. Negatively cooperative binding of melittin to neutral phospholipid vesicles. J. Mol. Struct. 2007;834-6:216-28.
[28] Torrens F, Castellano G, Campos A, Abad C. Binding of water-soluble, globular proteins to anionic model membranes. J. Mol. Struct. 2009;924-6:274-84.
[29] Torrens F, Castellano G. Comparative analysis of the electrostatics of the binding of cationic proteins to vesicles: Asymmetric location of anionic phospholipids, Anal. Chim. Acta 2009;654:2-10.
[30] Torrens F, Castellano G. Binding of mono, bi and tridomain proteins to zwitterionic and anionic vesicles: Asymmetric location of anionic phospholipids in mixed zwitterionic/anionic vesicles and cooperative binding. J. Life Sci. 2011;5:167-81.

[31] Torrens-Zaragozá F. Polymer bisphenol-A, the incorporation of silica nanospheres into epoxy–amine materials and polymer nanocomposites. Nereis 2011;2011(3):17-23.
[32] Torrens-Zaragozá F. Calculation of restricted volume for nanoparticles that can point. Nereis 2017;2017(9):25-38.
[33] Derjaguin B, Landau L. Theory of the stability of strongly charged lyophobic sols and of the adhesion of strongly charged particles in solution of electrolytes. Acta Physicochim. U. R. S. S. 1941;14:633-62.
[34] Verwey EJW, Overbeek JTG. Theory of the stability of lyophobic colloids: The interaction of sol particles having an electric double layer. Amsterdam: Elsevier; 1948.
[35] Overbeek JTG. Recent developments in the understanding of colloid stability. J. Colloid Interface Sci. 1977;58:408-22.
[36] Russel WB, Saville DA, Schowalter W. Colloidal dispersions. Cambridge (UK): Cambridge University Press; 1989.
[37] Flory PJ. Principles of polymer chemistry. Ithaca (NY): Cornell University; 1953.
[38] Mandelbrot BB. The fractal geometry of nature. New York: Freeman; 1983.
[39] Stauffer D, Aharony A. Introduction to percolation theory. London: Taylor & Francis; 1991.
[40] Shih WH, Shih WY, Kim SI, Liu J, Aksay IA. Scaling behavior of the elastic properties of colloidal gels. Phys. Rev. A 1990;42:4772-9.
[41] Narine SS, Marangoni AG. Fractal nature of fat crystal networks, Phys. Rev. E 1999;59:1908-20.
[42] Bocquet L, Trizac E, Aubouy M. Effective charge saturation in colloidal suspensions, J. Chem. Phys 2002;117:8138-52.
[43] Chapot D, Bocquet L, Trizac E. Interaction between charged anisotropic macromolecules: Application to rod-like polyelectrolytes. J. Chem. Phys. 2004;120:3969-82.
[44] Steinem C, Janshoff A, Galla HJ. Evidence for multilayer formation of melittin on solid-supported phospholipid membranes by shear-wave resonator measurements. Chem. Phys. Lipids 1998;95:95-104.
[45] Beschiaschvili G, Seelig J. Melittin binding to mixed phosphatidylglycerol/phosphatidylcholine membranes. Biochemistry 1990;29:52-8.
[46] Vogel H. Incorporation of melittin into phosphatidylcholine bilayers: Study of binding and conformational changes. FEBS Lett. 1981;134:37-42.
[47] Vogel H, Jähnig F. The structure of melittin in membranes. Biophys. J. 1986;50:573-82.
[48] Vogel H. Comparison of the conformation and orientation of alamethicin and melittin in lipid membranes, Biochemistry 1987;26:4562-72.
[49] Schwarz G, Beschiaschvili G. Thermodynamic and kinetic studies on the association of melittin with a phospholipid bilayer. Biochim. Biophys. Acta 1989;979:82-90.
[50] Adamson AW, Gast AP. Physical chemistry of surfaces. New York: Wiley; 1997.
[51] Seydel JK, Wiese M. Drug-membrane interactions: Analysis, drug distribution, modeling. Methods and principles in medicinal chemistry No. 18. Weinheim, Ger.: Wiley–VCH; 2002.
[52] Stankowski S. Surface charging by large multivalent molecules. Extending the standard Gouy–Chapman treatment. Biophys. J. 1991;60:341-51.

[53] Pérez-Payá E, Thiaudière E, Abad C, Dufourcq J. Selective labelling of melittin with a fluorescent dansylcadaverine probe using guinea-pig liver transglutaminase. FEBS 1991;278:51-4.
[54] Pérez-Payá E, Braco L, Abad C, Dufourcq J. High-performance liquid chromatographic separation of modified and native melittin following transglutaminase-mediated derivatization with a dansyl fluorescent probe. J. Chromatogr., A 1991;548:351-9.
[55] Pérez-Payá E, Porcar I, Gómez CM, Pedrós J, Campos A, Abad C. Binding of basic amphipathic peptides to neutral phospholipid membranes: A thermodynamic study applied to dansyl-labeled melittin and substance P analogues. Biopolymers 1997;42:169-81.
[56] Pérez-Payá E, Dufourcq J, Braco L, Abad C. Structural characterisation of the natural membrane-bound state of melittin: A fluorescent study of a dansylated analogue. Biochim. Biophys. Acta 1997;1329:223-36.
[57] Pott T, Maillet JC, Abad C, Campos A, Dufourcq J, Dufourc EJ. The lipid charge density at the bilayer surface modulates the effects of melittin on membranes. Chem. Phys. Lipids 2001;109:209-23.
[58] Pérez-Payá E, Ferrándiz C, Abad C. The amphipathic peptide melittin as a tool to study the membrane-dependent activation of tissue transglutaminase. Lett. Peptide Sci. 2002;8:69-76.